Proceedings of the ASME 2020 International Design Engineering Technical Conferences & Computers and Information in Engineering Conference
IDETC/CIE 2020
August 16-19, 2020, St. Louis, MO, USA

DETC2020/XXXX-XXXX

DRAFT: NEUROADAPTIVE CONTROLLER FOR PHYSICAL INTERACTION WITH AN OMNI-DIRECTIONAL MOBILE NURSE ASSISTANT ROBOT

Mohammad N. Saadatzi*
Next Generation Systems
Electrical and Computer Eng.
University of Louisville
Louisville, Kentucky 40208

Shamsudeen Abubakar
Next Generation Systems
Electrical and Computer Eng.
University of Louisville
Louisville, Kentucky 40208

Sumit Kumar Das
Next Generation Systems
Electrical and Computer Eng.
University of Louisville
Louisville, Kentucky 40208

M. Hossein Saadatzi
Next Generation Systems
Electrical and Computer Engineering
University of Louisville
Louisville, Kentucky 40208

Dan Popa
Next Generation Systems
Electrical and Computer Engineering
University of Louisville
Louisville, Kentucky 40208

ABSTRACT

Robot-assisted healthcare could help alleviate the shortage of nursing staff in hospitals and is a potential solution to assist with safe patient handling and mobility. In an attempt to off-load some of the physically-demanding tasks and automate mundane duties of overburdened nurses, we have developed the Adaptive Robotic Nursing Assistant (ARNA), which is a custom-built omnidirectional mobile platform with a 6-DoF robotic manipulator and a force sensitive walking handlebar. In this paper, we present a robot-specific neuroadaptive controller (NAC) for ARNA's mobile base that employs online learning to estimate the robot's unknown dynamic model and nonlinearities. This control scheme relies on an inner-loop torque controller and features convergence with Lyapunov stability guarantees. The NAC forces the robot to emulate a mechanical system with prescribed admittance characteristics during patient walking exercises and bed moving tasks. The proposed admittance controller is implemented on a model of the robot in a Gazebo-ROS simulation environment, and its effectiveness is investigated in terms of online learning of robot dynamics as well as sensitivity to payload variations.

INTRODUCTION

According to the US Bureau of Labor Statistics [1], registered nurses will be the largest labor pool in the US by 2022, and more than 1.1 million nursing positions have to be filled by then in order to avoid additional shortage. Robots are a potential solution in healthcare environments to assist with safe patient handling and mobility, thereby reducing the likelihood of workplace injuries. In recent years, robots have been used in hospitals to assist with surgical procedures, to deliver medications, to monitor patients, and to assist with daily hygiene [2]. For instance, nursing assistant robots with a human form factor have been employed to provide patient lift assistance to nurses and, hence, prevents lifting-related musculoskeletal injuries [3]. Other endeavors in the literature to assist nursing staff with physical tasks in healthcare environments include robotic patient lift

*Address all correspondence to this author (mn.saadatzi@louisville.edu).

FIGURE 1: ADAPTIVE ROBOTIC NURSING ASSISTANT (ARNA) INCLUDING AN OMNIDIRECTIONAL MOBILE PLATFORM, A 6-DOF MANIPULATOR, AND AN INSTRUMENTED HANDLEBAR.

and transfer [4] and robot-assisted dressing of patients [5].

In an attempt to off-load some of the physically-demanding tasks and automate mundane low-level duties of overburdened nurses, we have developed the Adaptive Robotic Nursing Assistant, ARNA, which is a service robot capable of navigating in cluttered hospital environments and performing automated nursing tasks. ARNA is a heavy-duty omnidirectional mobile robot constructed in-house with a customized 6-DoF robotic manipulator (Fig. 1). In this paper, we have developed a physical human-robot interaction (pHRI) strategy for the ARNA robot that interprets the force/torque readings from the instrumented handle bar and controls its motion based on a model-free admittance control scheme.

Admittance and impedance control are popular classes of implicit force control, and have been extensively studied in terms of stability and performance in robotic contact tasks [6, 7]. The preliminary goal in this control technique is to provide a stable contact by the robot's end effector during robot-environment contact or to prepare a natural physical human-robot interaction (pHRI), by regulating the mechanical compliance of the robot [7, 8]. In general admittance control, the tracking error dynamics are forced to follow a prescribed admittance model with virtual mass, stiffness, and damping coefficients, and, thereby enabling the robot to behave compliantly [9–11]. The admittance control technique, however, typically depends on a known dynamic model of the robot as well as the robot-environment contact characteristics [12]. In the case of ARNA, however, the system suffers from a highly-perturbed dynamics as the robot is subject to diverse slopes as well as uncertain and heavy payloads (e.g., hospital beds with bariatric patients atop, and riders with unknown weight). Furthermore, these payloads are exerted at different sides of the robot (e.g., heavy bed in the front, human rider at the back, and medical equipment around the robot). Such unbalanced payload distribution results in an unknown, time-varying center of gravity and, ultimately unbalanced load and frictional forces on each actuator. Additionally, nonlinearities caused by inherent flexibility/uncertainty in the handlebar-user linkage increase the overall model's perturbations. In the presence of these inaccuracies, relying on model-based controllers lead to performance deterioration and hence safety hazards (e.g., collision), unless conservatively-high controller gains are employed.

For guaranteed trajectory tracking in robots with nonlinearities and model uncertainties, various adaptive control algorithms have been employed based on, for instance, feedback linearization and computed torque control [13]. There also exist a number of efforts in the literature that successfully implemented neuroadaptive schemes to control robotic manipulators with modeling inaccuracies [14]. The pioneering work by Lewis [12] and colleagues proposed a neural network (NN) controller that tuned parameters of the closed-loop system's error dynamics to approach a desired dynamic model.

In this paper, we propose a robot-specific adaptive admittance controller for the ARNA robot's omnidirectional base that employs NN-based learning to online approximate the robot's unknown model and to cancel out its nonlinearities. This control scheme relies on an inner-loop torque controller that forces the robot to emulate a mechanical system with desired admittance characteristics, with convergence guarantees, in response to operator input forces/moments applied to ARNA's handlebar. The proposed admittance controller, which requires no prior information about the task or trajectory, enables a consistent performance of the robot from the operator's point of view, despite directional and dynamic nonlinearities of the robot. As such, this controller obviates the need for the operator to learn and compensate for task-specific model and uncertainties of the robot, thereby reducing the operator's cognitive and physical load.

SYSTEM DESCRIPTION

The ARNA robot has been developed to assist nursing staff through cooperation during physical activities (bed and cart pushing, item fetching, etc.) and to improve their productivity through automation of repetitive non-physical tasks (patient observation, vital signs measurements, etc.).

Omnidirectional Mobile Platform

ARNA's drive-train is composed of four Mecanum wheels, arranged in a longitudinal symmetrical layout [15], and are driven by four independently-controlled servo motors with angle, velocity, and torque feedback. The servo motors are coupled with the Mecanum wheels through right-angled high-ratio gearboxes, and are mounted to the four corners of the robot chassis (Fig. 2). This drive-train allows omnidirectional mobility and enables simultaneous and independent translational (forward/backward, sideways) and rotational maneuvers from any configuration, obviating the need for non-holonomic path plan-

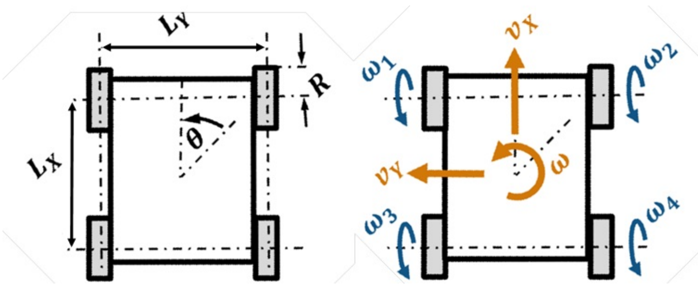

FIGURE 2: SCHEMATIC OF THE MOBILE PLATFORM WITH FOUR MECANUM WHEELS.

ning and control. Such omnidirectional mobility truly yields the user's navigational intent and is ideal for collision avoidance and navigating through congested hospital corridors in close proximity of humans.

Mecanum wheels are fairly traditional wheels which include a few rollers mounted around their perimeter. The rollers may be installed with various bias angles but they are usually mounted at a 45° angle to the plane of the wheel in contact with the ground. With a zero-roller-ground-slippage assumption, the inverse kinematics of the platform moving on a horizontal plane can be formulated as:

$$V_w = \begin{bmatrix} \omega_1 \\ \omega_2 \\ \omega_3 \\ \omega_4 \end{bmatrix} = J.V = \frac{1}{R} = \begin{bmatrix} 1 & -1 & -(L_X+L_Y)/2 \\ 1 & 1 & (L_X+L_Y)/2 \\ 1 & 1 & -(L_X+L_Y)/2 \\ 1 & -1 & (L_X+L_Y)/2 \end{bmatrix} \begin{bmatrix} v_X \\ v_Y \\ \omega \end{bmatrix} \quad (1)$$

where V_w is the wheels' velocity vector, J is the Jacobian matrix, $V = [v_X, v_Y, \omega]^T$ is the generalized velocity vector of center point of rotation [16]. In this equation, R is the Mecanum wheel radius, and L_X and L_Y are two parameters associated with the layout of the platform as shown in Fig. 2.

Instrumented Handlebar

At the rear end of the mobile platform, ARNA incorporates a handlebar. When ARNA is used as an ambulatory assistive device, this handlebar provides a physical support for patients to hold onto and maintain their balance while walking with the robot. In addition, this handlebar serves as ARNA's main human-machine interface (HMI) as it is instrumented with an industrial 6-axis force/torque sensor. When a patient holds onto this handlebar and applies force and moments, ARNA's main control unit interprets the force/torque measurements for his/her navigational intent, and moves the mobile platform accordingly based on an admittance controller scheme (as explained in the following section). This instrumented handlebar, along with the underlying admittance controller, provide an intuitive HMI for ARNA and a natural pHRI between ARNA and its users. Through this handlebar, a nurse can control the robot's motion when, for instance, manually moving heavy items, such as hospital beds and carts.

CONTROLLER FORMULATION

In an admittance controller, the objective is to produce robot's movement in response to sensed forces/torques. Admittance of a compliant mechanical structure is typically represented as a transfer function, G, which is the ratio of the structure's velocity to the forces/torques applied to the structure [17], as

$$G(s) = V(s)F^{-1}(s), \quad (2)$$

where F is the input forces/torques, V is the output velocity, and s is the complex frequency. A mechanical structure with a large admittance is easily set in motion with the application of small forces and torques; while a structure with a small admittance requires large acting forces and torques. In this study, an admittance-based interaction control scheme is developed for ARNA's mobile platform. In this scheme, ARNA moves in response to forces and torques applied by a user to its handlebar, and emulates a dynamic system with desired compliant characteristics. As depicted in Fig. 3, this control scheme includes a feed-forward admittance model and a closed-loop neuroadaptive controller. The admittance model generates the reference motion of the mobile platform in response to the human force/torque inputs, which is then converted to reference motion of each wheel using the robot's inverse kinematics given in (1). Finally, the neuroadaptive controller ensures the reference motion of each wheel is tracked, even in the presence of nonlinearities and uncertainties. The neuroadaptive inner-loop controller used in this study does not rely on any information about the feed-forward admittance model, enabling a decoupled design of the task-specific admittance model.

Prescribed Admittance Model

ARNA's mobile platform has three degrees of freedom (DoF); longitudinal, lateral, and rotational motions. Therefore, a 3-DoF decoupled mass-damper admittance model was developed for its motion, as below, prescribing its compliance behavior in each respective direction.

$$V(s) = G(s)F(s) = diag(G_x(s), G_y(s), G_\omega(s))F(s) = \\ diag(\frac{1}{(sM_x+D_x)}, \frac{1}{(sM_y+D_y)}, \frac{1}{(sM_\omega+D_\omega)}) \begin{bmatrix} f_X \\ f_Y \\ \tau_\omega \end{bmatrix} \quad (3)$$

where f_x and f_y are the forces applied to the handlebar in the x and y directions, respectively, and τ_z is the torque in the

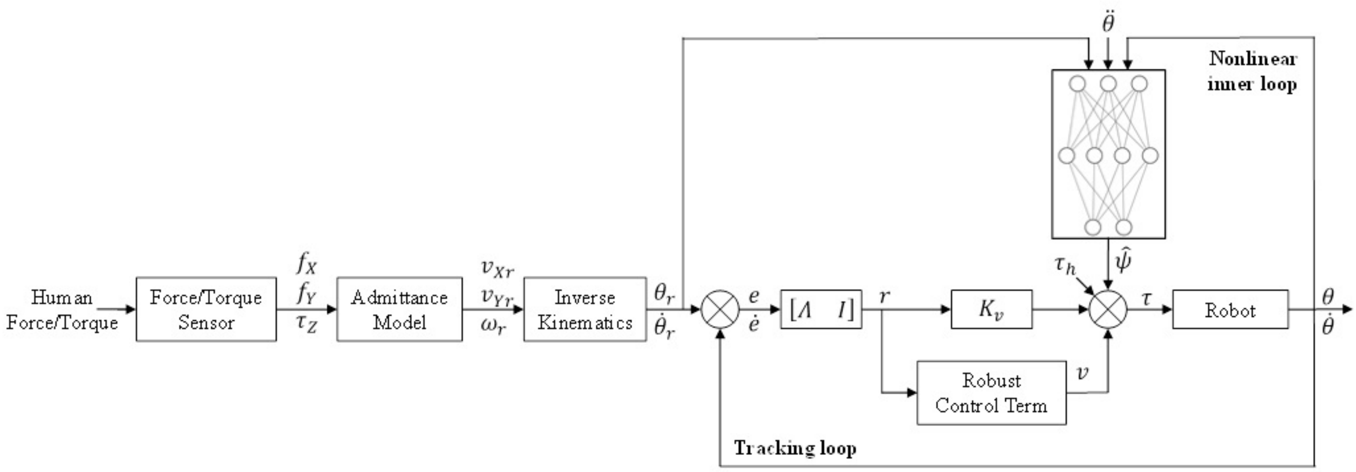

FIGURE 3: ADMITTANCE CONTROLLER INCLUDING FEED-FORWARD ADMITTANCE MODEL AND INNER-LOOP NEUROADAPTIVE CONTROLLER.

rotational direction. In this equation, M_i and $D_i, i \in \{x, y, \omega\}$, are the virtual inertial and damping coefficients of the admittance model, respectively, that are prescribed to achieve desired characteristics for force-to-motion conversion in each direction. For instance, the steady-state response of the admittance model in the longitudinal direction when a constant force f_x is applied to the handlebar is f_x/D_x. In other words, to achieve a steady-state forward velocity of $v_{x,ss}$, a constant pushing force of $D_x v_{x,ss}$ is required. Following this logic, the damping coefficients (i.e., D_x, D_y, and D_ω), determine the user's burden necessary for a target velocity in different directions. Similarly, the time constant of these transfer functions is $M_i/D_i, i \in \{x, y, \omega\}$. Therefore, by adjusting these virtual coefficients, we can alter both transient and steady-state response of the system, and arbitrarily shape the human-robot interaction dynamics. In practice, these design parameters are adjusted such that the velocities reach equilibrium as quickly as possible without oscillation, while minimizing the physical burden on the human user in order to offer maximal power assistance.

Time-domain output of this transfer function in response to the force/torque measurements is solved in real time and set as the desired velocities of the mobile platform. By solving the inverse kinematics of the mobile platform, presented in (1), we can obtain the desired actuator velocities. Such an admittance control scheme emulates a dynamic system with a desired, linear behavior, and induces a feeling in the user as if they are interacting with a mechanical system with those prescribed characteristics.

Neuroadaptive Controller

The origin of NNs-based system identification and closed-loop control systems goes back to the early 1990s through the seminal work by Narendra and Parthasarathy [18], where multilayer and recurrent networks, along with back-propagation techniques, were successfully used to control nonlinear dynamic systems. Since then, numerous studies have investigated internal stability and tracking performance guarantees of NNs-based control systems [19–21]. In the current study, we extend the neuroadaptive controller initially presented by Lewis and colleagues [14,20] to ARNA's mobile base in a joint trajectory tracking task. Below the formulation of this neuroadaptive controller, in the joint space, is discussed in short.

The robot's dynamics in the joint space is

$$H(\theta)\ddot{\theta} + C(\theta,\dot{\theta})\dot{\theta} + F(\dot{\theta}) + G(\theta) + \tau_d = \tau + \tau_h, \tag{4}$$

where θ is the robot's joint angles, H is the inertial/mass matrix, C is the Coriolis matrix, τ_d is the disturbance vector, τ is the control torque, τ_h is the user input, and F summarizes the friction forces.

The admittance model block, followed by the robot's inverse kinematics, determines the desired trajectory of each actuator (i.e., in the joint space) in response to the user forces and torques exerted to the ARNA's handlebar. Assuming the reference trajectory in the joint space, θ_r, is known, the trajectory-following error, e, and the sliding-mode error, r, are defined as

$$e = \theta - \theta_r, \tag{5}$$

$$r = \dot{e} - \Lambda e, \tag{6}$$

where Λ is a symmetric, positive-definite design matrix. Incorporating (5) and (6) in (4), the sliding-mode error dynamics is achieved as

$$\begin{aligned} &H(\theta)(\ddot{\theta}_r - \dot{r} + \Lambda\dot{e}) + C(\theta,\dot{\theta})(\dot{\theta}_r - r + \Lambda e) + F(\dot{\theta}) + \\ &G(\theta) + \tau_d = \tau + \tau_h, \end{aligned} \tag{7}$$

or more concisely as

$$H(\theta)\dot{r}+C(\theta,\dot{\theta})r+\psi(x)+\tau_d=\tau+\tau_h, \quad (8)$$

where $x=[e^T\,\dot{e}^T\,\theta_r^T\,\dot{\theta}_r^T\,\ddot{\theta}_r^T]$, and ψ is a nonlinear function that depends on the robot's uncertain parameters, defined as below.

$$\psi(x)=H(\theta)(\ddot{\theta}_r+\Lambda\dot{e})+C(\theta,\dot{\theta})(\dot{\theta}_r+\Lambda e)+F(\dot{\theta})+G(\theta) \quad (9)$$

As can be seen in (9), ψ is not a function of the prescribed admittance model parameters defined in (3), i.e., M_i and $D_i, i\in\{x,y,\omega\}$, which is different from typical admittance control schemes that rely on a model-following error as their trajectory-following objective [22].

The adaptive control scheme used in this study works based on an approximator that online-estimates the nonlinear ψ function given in (9) using a two-layer NN [23] as

$$\psi(x)=W^T\sigma(V^Tx)+\varepsilon, \quad (10)$$

where W and V are the ideal weights, σ is the activation function vector, and ε is the approximation error of the NN approximator. If the approximated function is denoted by $\hat{\psi}$, a control law can be formulated as

$$\tau=\hat{\psi}+K_vr-v(t), \quad (11)$$

where $K_v>0$ is a diagonal design parameter matrix, and $v(t)$ is a term added for robustification against inaccuracies, variabilities, and unstructured disturbances in the robot's model. If we define Z as

$$Z=\begin{bmatrix}\hat{W} & 0\\ 0 & \hat{V}\end{bmatrix}, \quad (12)$$

where $\hat{W}$ and $\hat{V}$ are the approximate NN weights, the signal $v(t)$ can be defined as

$$v(t)=-K_z(Z_B+\|\hat{Z}\|_F)r \quad (13)$$

where $K_z>0$ is a scalar gain, $\|.\|_F$ is the Frobenius norm operator, and Z_B is a constant positive scalar bound on the NN weights such that $\|\hat{Z}\|_F\le Z_B$.

Incorporating (11) in (8) yields the sliding-mode error dynamics as

$$H(\theta)\dot{r}+C(\theta,\dot{\theta})r+K_vr=\varepsilon+v+\tau_d \quad (14)$$

In practice, the ideal NN weights, W and V, are not known a priori, hence the following tuning algorithms are used in this study to compute and update $\hat{W}$ and $\hat{V}$ online.

$$\dot{\hat{W}}=A\hat{\sigma}r^T-A\hat{\sigma}'\hat{V}^Txr^T-\kappa A\|r|\hat{W} \quad (15)$$

$$\dot{\hat{V}}=Bx(\hat{\sigma}'^T\hat{W}r)^T-\kappa B\|r\|\hat{V} \quad (16)$$

$$\hat{\sigma}'=diag\{\sigma(\hat{V}^Tx)\}[I-diag\{\sigma(\hat{V}^Tx)\}] \quad (17)$$

In these update equations, A and B are two positive definite matrices, $\sigma(.)$ is the sigmoid activation function, and $\kappa>0$ is a small design parameter. Based on a rigorous Lyapunov argument in [14], it has been formally proven that the error signal defined in (5) converges zero when (15)-(17) are used as the tuning algorithm for the NN approximator. For in-depth discussion on the learning performance and proof of stability, refer to [14, 19, 20].

SIMULATION ENVIRONMENT

In order to investigate its effectiveness, the proposed controller was implemented on a numerical model of ARNA in Gazebo simulator. Gazebo is an open-source software capable of dynamic simulation of sensors, robots, and their interaction with the environment based on multiple physics engines. In Gazebo, a robot and its environment are typically defined using a Unified Robot Description Format (URDF) file written in XML format. To develop the Gazebo model of ARNA, we first created ARNA's CAD model in SolidWorks® and utilized a plugin to convert it to a URDF format. In this model, the Mecanum wheels were simulated using Gazebo's planar move plugin. Another plugin was also developed that computes propulsion forces/torques exerted on the robot chassis by the wheels in each simulation step. Subsequently, in order to obtain realistic dynamic behavior of the model, we tuned its physical parameters including mass/inertia of different elements and joint viscous/coulomb frictions, as well as the friction between the Mecanum wheels and the ground. Figure 4 depicts ARNA's model in Gazebo simulator.

To implement the admittance controller on the ARNA model, the Gazebo simulator was interfaced with Robot Operating System (ROS). ROS is a software framework for robot software development, and it provides services such as hardware abstraction, low-level device control, message-passing, and

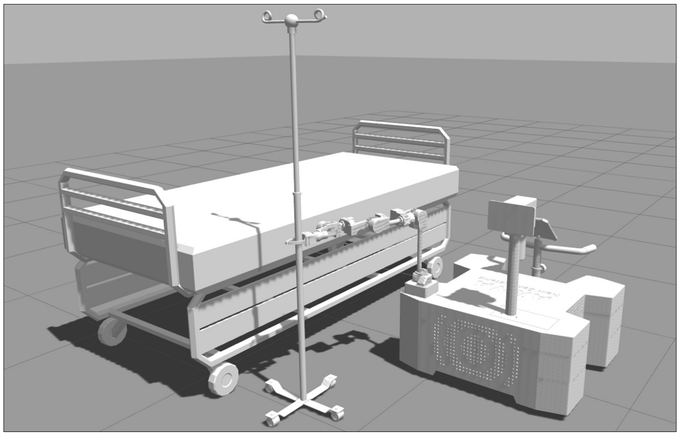

FIGURE 4: GAZEBO SIMULATION ENVIRONMENT INCLUDING ARNA, HOSPITAL BED, AND AN IV POLE.

package management. In this study, Gazebo 8.6 with ODE physics engine and ROS Kinetic on Ubuntu 16.0 were used. The Gazebo_ros_control plugin was utilized to facilitate communication between ROS packages by providing interfaces for robot joint actuation and robot data feedback. The Gazebo-ROS with the admittance controller was ran at 1 kHz.

RESULTS AND DISCUSSION

For the sake of safety, velocity of the ARNA mobile platform is electronically limited to 0.4 m/s, 0.4 m/s, and 0.2 rad/s, in longitudinal, lateral, and rotational directions, respectively. Considering these limits, the virtual inertia and damping coefficients of the admittance model were defined as tabulated in Tab. 1. These numbers were chosen so that the robot can start and stop gently, and reach the aforementioned desired steady-state values in each respective direction, without excessive burden (forces and torque) required from a human user. For example, with 15 N force applied by the user in the longitudinal direction, the robot gently reaches the steady-state longitudinal velocity of 0.4 m/s in 2.5 s. The overall compliance behavior of the robot, however, depends on the bandwidth of both the prescribed admittance model and the neuroadaptive controller. Therefore, in this study, the parameters of the inner loop controller were tuned such that its bandwidth was at least twice that of the admittance model, and hence, it could respond to the user input. These control parameters are summarized in Tab. 1.

TABLE 1: CONTROLLER PARAMETERS.

Parameter	Value
M_x, M_y	18.75 kg
D_x, D_y	37.5 Ns/m
M_ω	3 kgm^2
D_ω	6 Nm/rad
K_v	5 I$_4$ *
K_z	0.005
κ	0.07
Z_B	100
A	100 I$_4$ *
B	50 I$_4$ *

* I_4 is a 4x4 identity matrix

The presented admittance controller was implemented in our ROS-Gazebo simulation environment. The NN used had 2 layers, 21 inputs including bias, sigmoid activation functions, 15 neurons in the hidden layer, 4 outputs, and the weight matrices initialized with small random entries. The simulations included two set of experiments to examine efficacy of the proposed admittance controller and its inner-loop neuroadaptive controller.

In the first set, two scenarios were implemented in which ARNA moved in response to user force/torque inputs either (i) with no payload or (ii) while a 250-kg hospital bed was fastened to the robot front panel. The first scenario simulates a patient walking exercise or when a nurse operator docks the robot to a corner. In this scenario, the user input force/torque profile was defined such that ARNA moved along a circular path. In the second set of experiments, the robot moved along another path either (i) with no payload or (ii) with a 100-kg payload placed on the robot, which simulated a user riding the robot on its rear-end footrests. In all simulations, the robot was commanded to move starting from a standstill condition. Figures 5 and 6 illustrate the corresponding results including reference and actual velocities in joint space, and the control torques for each actuator.

The velocity tracking results in each of Figs. 5 show a good tracking performance. There are oscillations that settle within the first second of motion from rest in the with-payload condition in all the two motion profiles that do not occur in the no payload condition. These oscillations on the front wheels of the robot (i.e. wheel 1 and wheel 2 in Fig. 3, where the payload is connected) are larger than the oscillations at wheel 3 and wheel 4 (at the back of the robot). Based on the rigidity of ARNA robot mobile base, this observation suggests slipping of the wheels. Hence, the apparent oscillations do not entirely transfer to the user. This coupled with the fact that the oscillations are low-amplitude and short-duration suggest a smooth user experience for the user in the with-payload condition using NAC.

One limitation of this work is the absence of simulating the performance of the controller for complex reference wheel velocity trajectories with simultaneous components in all 3 Cartesian

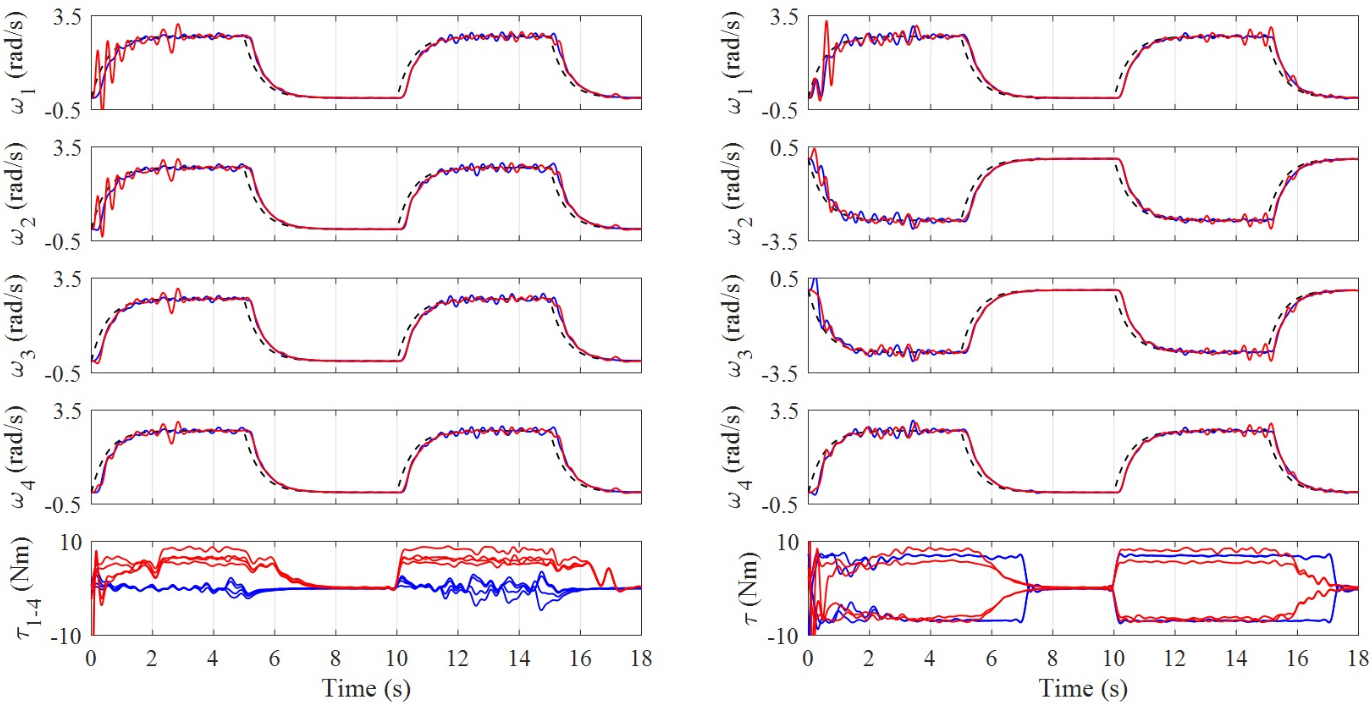

FIGURE 5: INDIVIDUAL JOINT VELOCITIES AND CONTROL TORQUE IN RESPONSE TO FORCE APPLIED TO THE HANDLEBAR IN LONGITUDINAL DIRECTION, I.E., $f_x = 10N$ (RIGHT PANEL), and LATERAL DIRECTION, I.E., $f_y = 10N$ (LEFT PANEL). THE DASHED LINE IS THE OUTPUT OF THE ADMITTANCE MODEL FOR EACH JOINT. THE BLUE TRAJECTORIES ARE FOR THE NO-PAYLOAD CONDITION, AND THE RED TRAJECTORIES ARE FOR THE WITH-PAYLOAD CONDITION.

axes. This was not done because of the Gazebo limitations in simulation of sideways motion of Mecanum wheels. To solve this problem, we intend to implement this simulation and the controller in V-REP [24], which is a simulation suite that facilitates simulation of such motion.

Generally, the results show the feasibility of the use and benefits of the NAC for the control of a mobile robot base. While there has been some work showing use of the NAC for a robotic arm [25,26], we believe this is the first use with a mobile robotic base. The use of NAC for a mobile base as presented here also provides a good platform for the integration of other machine learning based control approaches for use in multiuser pHRI in a clustered environment [27].

CONCLUSION

In this paper, we introduced the Adaptive Robotic Nursing Assistant, designed to assist nurses with some of their physically-demanding tasks. ARNA has several human-machine interfaces, such as a custom-built tablet interface as well as a handlebar instrumented with a 6-axis force/torque sensor. In this paper we paper investigated the characteristics of the physical HRI between users and the ARNA through its handlebar that is enhanced by a NNs-based admittance controller which offers guaranteed stability and convergence. This admittance controller is designed in two decoupled steps; (i) a feed-forward admittance model that prescribes the compliant behavior of the robot in response to human efforts, and (ii) a neuroadaptive inner-loop controller that learns and compensates the nonlinearities and un-modeled dynamics of the robot online. Through ROS-Gazebo simulations, we verified the effectiveness of the admittance controller in reducing sensitivity to the robot nonlinearities and inaccuracies, as well as the perturbations caused by substantial variation in payload condition.

In the future, we will implement the presented admittance controller on the actual robot and run experiments with human users with diverse physical and cognitive abilities.

ACKNOWLEDGMENT

This work was supported by National Science Foundation awards IIP #1643989, and OIA #1849213.

REFERENCES

[1] Bureau of Labor Statistics, 2018. *US Department of Labor, Occupational Outlook Handbook*.

[2] Kangasniemi, M., Karki, S., Colley, N., and Voutilainen, A., 2019. "The use of robots and other automated devices in nurses' work: An integrative review". *International journal of nursing practice,* ***25***(4), p. e12739.

[3] Hu, J., Edsinger, A., Lim, Y.-J., Donaldson, N., Solano, M., Solochek, A., and Marchessault, R., 2011. "An advanced medical robotic system augmenting healthcare capabilities-robotic nursing assistant". In IEEE international conference on robotics and automation, pp. 6264–6269.

[4] Liu, Y., Chen, G., Liu, J., Guo, S., and Mukai, T., 2018. "Biomimetic design of a chest carrying nursing-care robot for transfer task". In IEEE International Conference on Robotics and Biomimetics (ROBIO), pp. 45–50.

[5] Erickson, Z., Collier, M., Kapusta, A., and Kemp, C. C., 2018. "Tracking human pose during robot-assisted dressing using single-axis capacitive proximity sensing". *IEEE Robotics and Automation Letters,* ***3***(3), pp. 2245–2252.

[6] Calanca, A., Muradore, R., and Fiorini, P., 2015. "A review of algorithms for compliant control of stiff and fixed-compliance robots". *IEEE/ASME Transactions on Mechatronics,* ***21***(2), pp. 613–624.

[7] Hogan, N., 1984. "Impedance control: An approach to manipulation". In American control conference, pp. 304–313.

[8] Anderson, R. J., and Spong, M. W., 1988. "Hybrid impedance control of robotic manipulators". *IEEE Journal on Robotics and Automation,* ***4***(5), pp. 549–556.

[9] Tsuji, T., and Tanaka, Y., 2005. "Tracking control properties of human-robotic systems based on impedance control". *IEEE Transactions on systems, man, and cybernetics-Part A: Systems and Humans,* ***35***(4), pp. 523–535.

[10] Clover, C. L., Luecke, G. R., Troy, J. J., and McNeely, W. A., 1997. "Dynamic simulation of virtual mechanisms with haptic feedback using industrial robotics equipment". In Proceedings of IEEE International Conference on Robotics and Automation, Vol. 1, pp. 724–730.

[11] Duchaine, V., and Gosselin, C., 2009. "Safe, stable and intuitive control for physical human-robot interaction". In IEEE International Conference on Robotics and Automation, pp. 3383–3388.

[12] Kazerooni, H., Sheridan, T., and Houpt, P., 1986. "Robust compliant motion for manipulators, part i: The fundamental concepts of compliant motion". *IEEE Journal on Robotics and Automation,* ***2***(2), pp. 83–92.

[13] Lewis, F. L., Dawson, D. M., and Abdallah, C. T., 2003. *Robot manipulator control: theory & practice*. CRC Press.

[14] Lewis, F., Jagannathan, S., and Yesildirak, A., 1998. *Neural network control of robot manipulators and non-linear systems*. CRC Press.

[15] Wang, Y., and Chang, D., 2009. "Motion performance analysis and layout selection for motion system with four mecanum wheels". *Journal of mechanical engineering,* ***45***(5), pp. 307–310.

[16] Tătar, M. O., Popovici, C., Mândru, D., Ardelean, I., and Pleşa, A., 2014. "Design and development of an autonomous omni-directional mobile robot with mecanum wheels". In IEEE International Conference on Automation, Quality and Testing, Robotics, pp. 1–6.

[17] Newman, W. S., 1992. "Stability and Performance Limits of Interaction Controllers". *Journal of Dynamic Systems, Measurement, and Control,* ***114***(4), 12, pp. 563–570.

[18] Kumpati, S. N., Kannan, P., et al., 1990. "Identification and control of dynamical systems using neural networks". *IEEE Transactions on neural networks,* ***1***(1), pp. 4–27.

[19] Lewis, F. L., Liu, K., and Yesildirek, A., 1995. "Neural net robot controller with guaranteed tracking performance". *IEEE Transactions on Neural Networks,* ***6***(3), pp. 703–715.

[20] Lewis, F. L., Yesildirek, A., and Liu, K., 1996. "Multilayer neural-net robot controller with guaranteed tracking performance". *IEEE Transactions on Neural Networks,* ***7***(2), pp. 388–399.

[21] Polycarpou, M. M., 1996. "Stable adaptive neural control scheme for nonlinear systems". *IEEE Transactions on Automatic control,* ***41***(3), pp. 447–451.

[22] Gribovskaya, E., Kheddar, A., and Billard, A., 2011. "Motion learning & adaptive impedance for robot control during physical interaction with humans". In IEEE International Conference on Robotics and Automation, pp. 4326–4332.

[23] Yesildirek, A., and Lewis, F. L., 1994. "Feedback linearization using neural networks". In IEEE International Conference on Neural Networks (ICNN'94), Vol. 4, pp. 2539–2544.

[24] Rohmer, E., Singh, S. P., and Freese, M., 2013. "V-rep: A versatile and scalable robot simulation framework". In IEEE/RSJ International Conference on Intelligent Robots and Systems, pp. 1321–1326.

[25] Ranatunga, I., Cremer, S., Lewis, F. L., and Popa, D. O., 2015. "Neuroadaptive control for safe robots in human environments: a case study". In IEEE International Conference on Automation Science & Engineering, pp. 322–327.

[26] Das, S. K., Wijayasighe, I., Saadatzi, M. N., and Popa, D. O., 2018. "Whole body human-robot collision detection using base-sensor neuroadaptive interaction". In IEEE 14th International Conference on Automation Science and Engineering (CASE), pp. 278–283.

[27] Cremer, S., Das, S. K., Wijayasinghe, I. B., Popa, D. O., and Lewis, F. L., 2019. "Model-free online neuroadaptive controller with intent estimation for physical human–robot interaction". *IEEE Transactions on Robotics*.